ELSEVIER

Journal of Alloys and Compounds 235 (1996) 53–58

Journal of ALLOYS AND COMPOUNDS

Kinetic study of the growth of the $(Bi,Pb)_2Ca_2Sr_2Cu_3O_{10}$ phase from calcined precursor powders

J.-C. Grivel, R. Flükiger

Département de Physique de la Matière Condensée, Université de Genève, CH-1211 Genève 4, Switzerland

Received 21 July 1995

Abstract

The phase formation kinetics of the Bi,Pb(2223) phase in powders with two different nominal compositions has been studied. An analysis of the Bi,Pb(2223) phase evolution using the Avrami relation for isothermal phase transformations revealed a two-stage process with a marked change of the n-exponent during the course of the Bi,Pb(2223) phase formation after about 12 h sintering. The activation energy for this formation and the value of the Avrami exponent were found to be related to the extent of partial melting occurring in the precursor powders.

Keywords: Bi–Pb–Sr–Ca–Cu–O system; Phase formation kinetics; Activation energy

1. Introduction

In recent years, much effort has been focused on the synthesis of the $(Bi,Pb)_2Sr_2Ca_2Cu_3O_{10}$ phase (Bi,Pb(2223)). This interest is essentially due to the possibility of using it in high j_c superconducting tapes.

A detailed knowledge of the formation mechanism of the Bi,Pb(2223) phase is essential in order to improve the preparation procedure of this compound. The Avrami relation for isothermal transformations [1] has been used by various authors to study the kinetics of the Bi,Pb(2223) phase formation with contradictory results [2–7]. In particular, the reported n-exponents and the activation energies relating to the formation of the Bi,Pb(2223) phase differ greatly among the various publications.

In this paper we report our investigations of the Bi,Pb(2223) phase formation kinetics performed on two different nominal compositions close to the ideal Bi,Pb(2223) stoichiometry. It appears that the nominal composition significantly influences the value of the activation energy. Furthermore, it will be shown that the n-exponent presents a marked change after about 12 h sintering in both investigated compositions.

2. Experimental details

The powder mixtures used in this work consisted of commercially available coprecipitated oxalates. The investigated nominal compositions were: $Bi_{1.72}Pb_{0.34}Sr_{1.83}Ca_{1.97}Cu_{3.13}O_x$ (A) and $Bi_{1.83}Pb_{0.33}Sr_{1.93}Ca_{1.93}Cu_{3.00}O_x$ (B). All powders were heat-treated in the same way. The oxalates were first dehydrated and decomposed at 750°C. The resulting powders were then pressed into pellets and calcined at 800°C for 48 h with one intermediate grinding. The precursor powders thus obtained were pressed into pellets of about 45 mg with 3.6 mm diameter and about 1 mm thickness under a pressure of 1.0 GPa. The sintering treatments were performed in air. The temperature was controlled within ±1°C using a calibrated Pt/Pt–Rh thermocouple positioned close to the samples. At the end of each treatment, the alumina crucible containing the samples was removed directly in air. No further annealing was performed prior to measurements. From comparisons of pellets quenched in air and into oil, we found no significant variations in the Bi,Pb(2223) and $Bi_2Sr_2CaCu_2O_8$ (Bi(2212)) phase contents. For this reason, air-quenching was used for the present investigation.

X-ray diffraction (XRD) patterns of powdered samples were recorded on a Philips θ–2θ diffractometer (Ni filtered Cu Kα radiation). DTA measurements with a heating rate of 120°C h^{-1} were performed in a SETARAM TAG 24 thermal analyzer using Al_2O_3 as reference in flowing synthetic air (O_2 21%, N_2 bal-

SSDI 0925-8388(95)02149-3

ance). The samples consisted of powders (ca. 80 mg) pressed into pellets with 3.6 mm diameter under a pressure of 0.5 GPa.

2.1. Data analysis

The kinetics of conversion of the Bi,Pb(2223) phase from the precursor powders was analyzed by the Avrami relation for isothermal phase transformations [1]. The Avrami equation, which has been found to be well suited to describe the Bi,Pb(2223) phase formation [5], is expressed as follows:

$$V = 1 - \exp(-kt^n) \quad (1)$$

where V is the volume fraction of the sample transformed into Bi,Pb(2223), k is the rate constant, t the equilibration time at the reaction temperature and n an exponent (Avrami exponent) dependent on the nature and the characteristics of the transformation. According to Rao and Rao [8], in the case of diffusion-controlled transformations, the exponent n can take the following values:

(i) $n = 2.5$—initial growth of particles nucleated at constant rate;

(ii) $n = 1.5$—initial growth of particles nucleated only at the start of the transformation;

(iii) $n = 1$—growth of isolated plates or needles of finite size;

(iv) $n = 0.5$—thickening of plates after their edges have impinged.

Note that the value of n is subjected to variations with changes in the temperature as a consequence of slight variations in the transformation conditions. This makes direct comparison of the n values determined by different authors under the various experimental conditions difficult.

In Eq. (1), the reaction rate obeys an Arrhenius type of relation:

$$k = k_0 \exp(-E_{act}/RT) \quad (2)$$

where k_0 is a constant, E_{act} is the activation energy for the phase formation, R is the gas constant and T is the absolute temperature.

The theoretical analysis of Avrami is based on the assumption that germ nuclei from which the new phase is nucleated are already present and randomly distributed in the sample at the time taken as $t = 0$. If the precursor powders have been previously calcined, as is the case in the present investigation, at temperatures lower than the Bi,Pb(2223) phase formation temperature, this assumption is not fulfilled. In such a case, the use of an immersion heating method would require the introduction of an 'incubation time' in the subsequent analysis of the data, which is not very well defined. On the contrary, it can be reasonably assumed that the use of a heating ramp that ends above the minimum temperature at which the Bi,Pb(2223) phase forms, results in samples containing germ nuclei of the high-T_c phase at $t = 0$, provided this time is taken as that of the end of the heating ramp. However, it must be emphasized that too slow a heating ramp can lead to systematic errors in the subsequent analysis if it results in the formation of a significant amount of the new phase before reaching the equilibration temperature.

The heat treatments performed in the present investigation comprise a temperature ramp with a final rate of 30°C h^{-1} above 800°C. This kind of treatment does not result in the formation of a detectable amount of Bi,Pb(2223) phase up to the equilibration temperature, owing to its extremely slow formation rate. Indeed, the samples were only exposed for a short period of time to temperatures at which the Bi,Pb(2223) phase can form before reaching the sintering temperature.

In order to determine the fractional volume v of the Bi,Pb(2223) phase relative to that of the Bi(2212) phase in each sintered pellet, an empirical correlation curve, which related the fractional volume v to the XRD patterns was established by use of mixtures of standard powders of separately prepared Bi(2212) and Bi,Pb(2223) phases. The impurity content of these standard powders was determined approximately by optical microscopy (about 5 vol.% in Bi(2212) and about 10 vol.% in Bi,Pb(2223)) and was taken into account. The reflections selected for the determination of v were: $(002)_{2223}$, $(00\underline{1}0)_{2223}$, $(002)_{2212}$ and $(008)_{2212}$. These were chosen because a strong texture of both phases was produced owing to the deposition of a thin layer of powder on the flat sample holder used for XRD measurements, resulting in a very strong intensity for the $(00l)$ reflections. In addition, reflections $(002)_{2223}$ and $(002)_{2212}$ hardly overlap each other, which is also the case of $(008)_{2212}$ and $(00\underline{1}0)_{2223}$ with the difference that these lines lie in an angular interval where reflections other than $(00l)$ of both phases occur. Nevertheless, the intensity of these latter reflections is small and the texturing of the powders further ensures that they do not contribute significantly to the integrated intensity of the $(008)_{2212}$ and $(00\underline{1}0)_{2223}$ reflections.

In order to extract quantitative information about the kinetics of the Bi,Pb(2223) phase formation from the precursor powders, the variation of the sample volume occupied by phases other than Bi,Pb(2223) and Bi(2212) must be taken into account. Since our nominal compositions do not result in pure Bi,Pb(2223) phase, a non-negligible volume of secondary phases is present in the samples even after completion of the reaction. The corresponding volume has to be subtracted from the total sample volume. In

the present case, the relevant parameter is the difference between the volume of the phases other than Bi(2212) and Bi,Pb(2223) at the beginning and after completion of the reaction. These volume fractions were obtained from polished sections of selected pellets observed by scanning electron microscopy. Computer analysis of digitized images showed that the total volume fraction of the samples occupied by those secondary phases typically decreased by 20% during the reaction. This variation has to be taken into account in order to obtain the total Bi,Pb(2223) transformed volume fraction V from the value v determined by use of the calibration curve.

3. Results and discussion

After calcination at 800°C, the XRD patterns of both calcined precursor powders are essentially similar. The Bi(2212) phase is prominent, while CuO and Ca_2PbO_4 are clearly visible. Some faint lines of other phases, such as $Bi_2(Ca,Sr)_2CuO_x$ (Bi(2201)) and $(Ca,Sr)_2CuO_3$, are also detected. Slight variations in the relative intensities of the reflections of the various compounds are found in the XRD patterns of the calcined powders with the two investigated nominal compositions (listed in Table 1). This reflects changes in the relative proportions of the phases formed during the calcination step. Nevertheless, the phases detected by XRD were the same in both samples.

3.1. DTA measurements

The DTA measurements performed on the calcined powders are shown in Fig. 1. The powder of composition A clearly reveals two endothermic peaks between 840 and 900°C, confirming the shape reported in the literature [9–11]. The endothermic reaction responsible for the peak with the extrapolated $T_{onset} \cong 857$°C corresponds to the partial melting of the precursor powders. In the case of composition B, the intensity of this partial melting peak (I in Fig. 1) is lower, while its temperature, determined as illustrated in Fig. 1 for powder A, is similar to that of composition A within ±2°C. These features indicate that the amount of liquid phase available during the sintering will be higher in powder A, providing samples of both compositions are sintered at the same temperature.

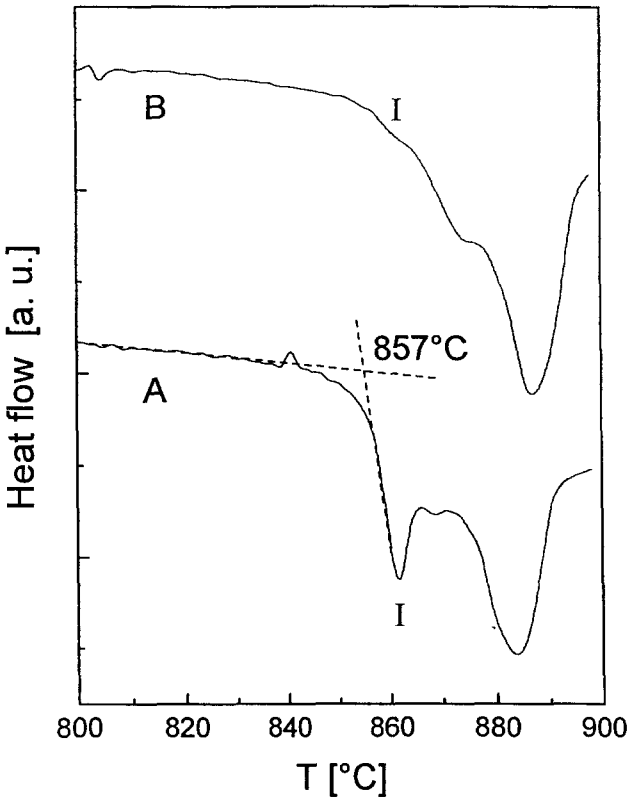

Fig. 1. DTA measurements performed on pellets of the calcined precursor powders.

It must be emphasized that the true onset of partial melting, which corresponds to the beginning of the downwards deviation from the base line in the DTA measurements, occurs at about 840°C for both compositions.

3.2. Phase formation kinetics

In order to study the Bi,Pb(2223) phase formation kinetics, pellets of both compositions were sintered at 857°C for various durations and air-quenched. This sintering temperature was selected since it lies in the temperature range where the highest amounts of Bi,Pb(2223) phase are formed, without resulting in a contamination by the Al_2O_3 crucible.

Fig. 2 shows the time variation of the volume fraction of the Bi,Pb(2223) phase in both compositions as determined from the XRD patterns following the procedure described in the experimental section.

Figs. 3 and 4 present the plots of $\ln[-\ln(1-V)]$ against $\ln(t)$ for the pellets of the nominal composi-

Table 1
Nominal compositions, n values ($n_1 = t < 12$ h, $n_2 = 12 < t < 35$ h) and activation energies for the formation of Bi,Pb(2223)

Composition	Bi:Pb:Sr:Ca:Cu at. ratio	n_1	n_2	E_{act} kJ mol^{-1}
A	1.72:0.34:1.83:1.97:3.13	1.5 ± 0.2	0.85 ± 0.08	500 ± 50
B	1.83:0.33:1.93:1.93:3.00	1.2 ± 0.2	0.63 ± 0.08	750 ± 50

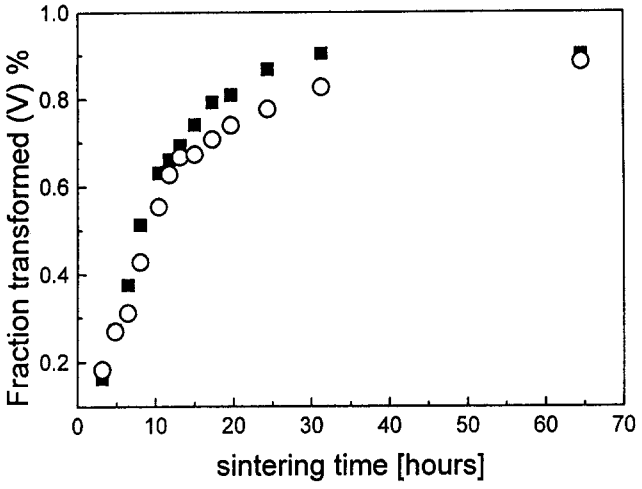

Fig. 2. Transformed volume fraction V of the Bi,Pb(2223) phase in the pellets sintered at 857°C as a function of sintering time: (■) composition A, (○) composition B.

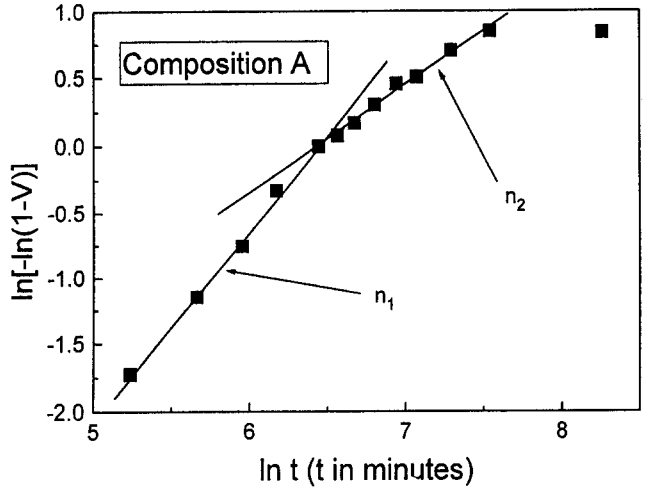

Fig. 3. $\ln[-\ln(1-V)]$ vs. $\ln(t)$ plot for pellets of composition A sintered at 857°C.

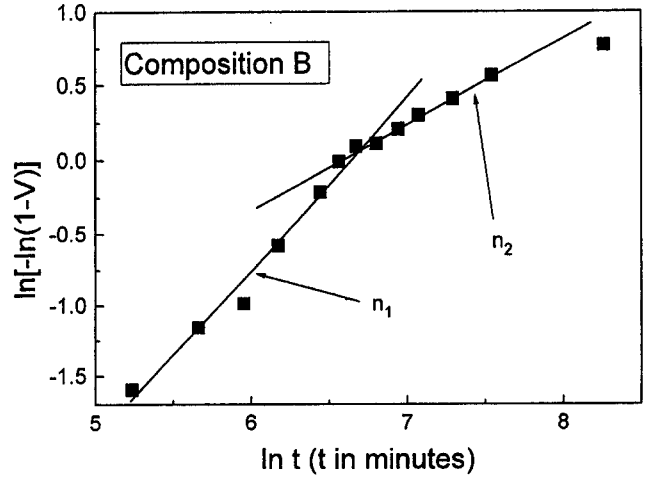

Fig. 4. $\ln[-\ln(1-V)]$ vs. $\ln(t)$ plot for pellets of composition B sintered at 857°C.

tions A and B respectively sintered at 857°C in air. Both graphs present three distinct regions. At short sintering times ($t < 12$ h) the slope is the highest (n_1 in Figs. 3 and 4) and n takes the values 1.5 and 1.2 for powders A and B respectively. For $12 < t < 35$ h, n is situated near 0.75 (n_2 in Figs. 3 and 4). For prolonged sintering the value of $\ln[-\ln(1-V)]$ in powders A and B reaches a plateau, indicating that the formation reaction is close to completion in these powders for sintering times longer than 35 h under the present experimental conditions. The values taken by n, which are reported in Table 1, do not correspond strictly to one of those typical for the types of transformation listed in the data analysis section. This fact is not surprising since some of them are likely to occur in a mixed way. The values of the exponent n for the first segment of the $\ln[-\ln(1-V)]$ vs. $\ln(t)$ plots are probably not reflecting the initial process of the transformation since we were not able to detect volume fractions of the Bi,Pb(2223) phase lower than 10% with accuracy. It is not excluded that a different behavior could take place at shorter sintering times ($t < 3$ h). In particular, the introduction of Pb into the Bi(2212) phase [10,12] is likely to have an influence at the onset of the reaction. The initial slopes for both compositions yield n values (n_1) close to 1.5, thereby indicating that at this stage of the reaction the Bi,Pb(2223) grains grow essentially from particles nucleated at the beginning of the transformation, i.e. essentially during the end of the heating ramp and/or the first hours of reaction. In this period ($3 < t < 12$ h), there is no more formation of a significant amount of germ nuclei. The previously formed germ nuclei are progressively activated to become growth nuclei for the grains of the Bi,Pb(2223) phase.

The n values for medium sintering times (n_2) are situated between 0.5 and 1. It is well known that the crystallites of the Bi,Pb(2223) phase have a platelet-like shape with high aspect ratio. This suggests that an n-value of 1 could be expected. Nevertheless, $n = 1$ would represent a pure two-dimensional growth without a contribution from thickening of crystallites. The simultaneous growth of Bi,Pb(2223) platelets together with their thickening, even if the relative importance of this last effect is rather small, will result in a lowering of the n value. Thus, after about 12 h sintering, the preformed nuclei have been almost completely activated to growth nuclei and/or ingested by the growing Bi,Pb(2223) grains.

Recently, Bian et al. [13] reported TEM investigations of Bi(2212) and Bi,Pb(2223) grains at the beginning of the Bi,Pb(2223) phase formation. They found that intergrowths consisting of alternate stackings of one half each of the Bi(2212) and the Bi(2223) unit cell along the [001] direction were present in the grains during the early stages of the transformation. It

is not excluded that such structures could be related to the germ nuclei of the Bi,Pb(2223) phase.

The n-values obtained for $t > 12$ h, i.e. above the kink in Figs. 3 and 4, present an interesting difference between the two compositions: $n_A = 0.85 > n_B = 0.63$. A comparison of this difference with the DTA traces shown in Fig. 1 indicates that the n-value is proportional to the intensity of the partial melting peak recorded in the precursor powders under the DTA measurement conditions. This suggests that a higher amount of liquid phase tends to promote the bidimensional growth of the Bi,Pb(2223) platelets relative to their thickening.

Among the kinetic studies performed on the formation of the Bi,Pb(2223) phase, some have been performed on Ag-sheathed tapes [5]. The n-values thus obtained are possibly influenced by the presence of Ag, as suggested by the study of Chiu et al. [6]; they will not, therefore, be quantitatively compared with those found in the present work.

A change in the n value during the formation of the Bi,Pb(2223) phase had been suggested by Kanai et al. [2], who used melt-quenched samples with $Bi_2Pb_{0.4}Sr_2Ca_2Cu_3O_y$ as a nominal composition. The initial value of n was 1.5 and changed to 0.5 after about 12 h annealing at 850°C in Ar–7.6%O_2 atmosphere. The authors attributed this variation to a change in the sample density during the process, without interpreting the values of the n exponent. Nevertheless, these results are very similar to ours in spite of the different ways of calculating the volume fraction of the Bi,Pb(2223) phase (magnetic measurements were used in Ref. [2]) and the fact that their $\ln[-\ln(1-V)]$ vs. $\ln(t)$ plot contained only four points. It is also remarkable that their $t = 12$ h for the change of slope is in agreement with our observations.

On bulk Ag-free samples, Kao et al. [7] obtained a value of $n = 1.1$ for a nominal composition $Bi_{1.7}Pb_{0.4}Sr_{1.6}Ca_{2.4}Cu_{3.6}O_y$ sintered at 853°C. However, these authors did not observe a change in the value of n during the Bi,Pb(2223) phase formation. Nevertheless, their $\ln[-\ln(1-V)]$ vs. $\ln(t)$ plot also contained only four points; therefore, this n-value of 1.1 could result from an averaging. In contrast, Zhu and Nicholson [3] studied a nominal composition corresponding to $Bi_{1.84}Pb_{0.34}Sr_{1.91}Ca_{2.03}Cu_{3.06}O_{10-y}$. They obtained n-values between 0.43 and 0.79 for sintering temperatures ranging from 840 to 870°C and $7.5 < t < 90$ h. These values are, to a first approximation, consistent with our measurements for medium sintering times ($12 < t < 35$ h).

3.3. Activation energy

The activation energy for the formation of the Bi,Pb(2223) phase was obtained by measuring the volume fraction of the high-T_c compound as a function of sintering temperature for a fixed sintering time, which was chosen as 17 h. The activation energies were extracted from $\ln[-\ln(1-V)]$ vs. $1/T$ plots, as shown in Fig. 5 for composition A. The values are listed in Table 1.

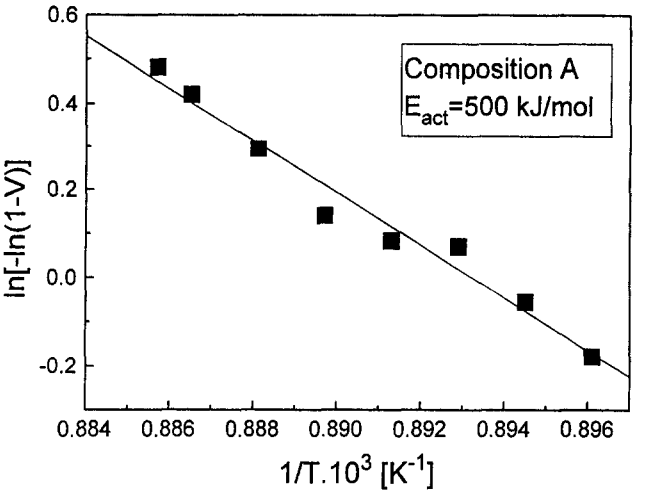

Fig. 5. $\ln[-\ln(1-V)]$ vs. $1/T$ plot for pellets of composition A sintered for 17 h at various temperatures.

Whereas the n-values indicate that in the two investigated compositions the growth of the Bi,Pb(2223) platelets is of similar nature, there is a strong variation among the E_{act} of the different powders. The values of E_{act} measured on both samples also show a relation with the intensity of the partial melting peak of the DTA curves. It appears that a higher amount of liquid phase results in a lower activation energy for the formation of the Bi,Pb(2223) phase.

High et al. found an activation energy for the growth of non-superconducting phases of about 510 kJ mol^{-1} in Ag-sheathed tapes sintered in 0.075 atm O_2 [14]. They compared this value with that obtained by Luo et al. [5] under similar conditions for the formation of the Bi,Pb(2223) phase in tapes (about 1500 kJ mol^{-1} according to Ref. [14]) and concluded that the reactions producing non-superconducting phases should be kinetically more favored than the Bi,Pb(2223) formation reaction. Nevertheless, the nominal compositions of the precursor powders used in these two publications were not the same: $Bi_{1.8}Pb_{0.4}Sr_2Ca_{2.2}Cu_3O_x$ [14] and $Bi_{1.7}Pb_{0.3}Sr_{1.9}Ca_2Cu_{3.1}O_x$ [5]. The significant differences found in the values of the activation energy for the formation of the Bi,Pb(2223) phase from precursors with slightly different nominal compositions, as shown in Table 1, show that care must be taken when comparing the kinetic characteristics of powders having different overall compositions. Our results suggest that the nominal composition of the precursor pow-

ders can be adjusted in order to decrease the activation energy for the formation of the Bi,Pb(2223) phase and possibly to favor the growth of this compound relative to that of non-superconducting phases. Nevertheless, a definitive answer to this last question would require a simultaneous study of the kinetics of the Bi,Pb(2223) and the non-superconducting phases formation as a function of the nominal composition, which was beyond the scope of the present investigation.

4. Conclusion

An analysis of the Bi,Pb(2223) phase formation kinetics by use of the Avrami relation for isothermal transformations revealed that, for each investigated nominal composition, the Bi,Pb(2223) phase is characterized by an initial growth which can be described as the growth of particles nucleated at the start of the transformation. After about 12 h sintering, the transformation mechanism changes to a mixed two-dimensional growth and thickening of the Bi,Pb(2223) platelets without further activation of germ nuclei into growth nuclei. The two-dimensional growth contribution to the value of the exponent n of the Avrami relation is higher in the powders which present the more prominent partial melting reaction. The characteristics of the formation kinetics for sintering times shorter than 3 h could not be found owing to the fact that the amount of Bi,Pb(2223) phase formed in the pellets was too low to accurately determine its proportion from X-ray measurements.

The activation energies related to the formation of the Bi,Pb(2223) phase were found to be significantly different in the two investigated nominal compositions. The value of this E_{act} seems to be related to the extent of partial melting occurring in the precursor powders. This feature could be the origin of the discrepancies found in the literature about the E_{act} obtained from different powder compositions.

Acknowledgements

The authors acknowledge the financial support of the Swiss National Foundation (PNR 30) and of BRITE-EURAM Project No. BRE2 CT92 0229.

References

[1] M. Avrami, *J. Chem. Phys., 7* (1939) 1103.
[2] T. Kanai, T. Kamo and S.P. Matsuda, *Jpn. J. Appl. Phys., 28* (1989) L2188.
[3] W. Zhu and P.S. Nicholson, *J. Mater. Res., 7* (1992) 38.
[4] J.S. Luo, N.M. Merchant, E. Escorcia-Aparicio, V.A. Maroni, D.M. Gruen, B.S. Tani, G.N. Riley, Jr. and W.L. Carter, *IEEE Trans. Appl. Supercond., 3* (1993) 972.
[5] J.S. Luo, N.M. Merchant, V.A. Maroni, D.M. Gruen, B.S. Tani, W.L. Carter and G.N. Riley Jr., *Appl. Supercond., 1* (1993) 101.
[6] Y.D. Chiu, C.H. Kao, T.S. Lei and M.K. Wu, *Physica C, 235–240* (1994) 485.
[7] C.H. Kao, Y.D. Chiu, S.L. Dung, L.C. Lee, T.S. Lei and M.K. Wu, *Mater. Lett., 20* (1994) 83.
[8] C.N.R. Rao and K.J. Rao, *Phase Transitions in Solids*, McGraw-Hill, 1978.
[9] T. Hatano, K. Aota, S. Ikeda, K. Nakamura and K. Ogawa, *Jpn. J. Appl. Phys., 27* (1988) L2055.
[10] J.-C. Grivel, A. Jeremie, B. Hensel and R. Flükiger, *Supercond. Sci. Technol., 6* (1993) 725.
[11] K. Aota, H. Hattori, T. Hatano, K. Nakamura and K. Ogawa, *Jpn. J. Appl. Phys., 28* (1989) L2196.
[12] N. Fukushima, H. Niu, S. Nakamura, S. Takeno, M. Hayashi and K. Ando, *Physica C, 159* (1989) 777.
[13] W. Bian, Y. Zhu, Y.L. Wang and M. Suenaga, *Physica C, 248* (1995) 119.
[14] Y.E. High, Y. Feng, Y.S. Sung, E.E. Hellstrom and D.C. Larbalestier, *Physica C, 220* (1994) 81.